

CHAPTER 10

SUMMARY AND CONCLUSIONS

10. SUMMARY AND CONCLUSIONS

Many existing pharmaceuticals are rendered ineffective in the treatment of cerebral diseases due to our inability to effectively deliver and sustain them within the brain. The major formidable obstacles for treating brain tumors include the drug delivery to the brain due to the presence of blood brain barrier (BBB), blood cerebrospinal fluid barrier and the brain tumor barrier. The BBB comprising of the endothelial cells forming tight junctions separates brain from the systemic circulation, thereby restricting delivery of therapeutics to brain. Further, the P-glycoprotein (Pg-P) abundant at the luminal membrane of BBB; remove the drugs before they penetrate brain parenchyma.

A brain tumor is a mass of cells that have grown and multiplied uncontrollably. Primary brain tumors originate in brain and may be benign with definite boundaries or malignant that spread to other parts of body. Metastatic (or secondary) brain tumors come from cancer cells in another part of the body. The diseased cells spread to the brain by moving through the bloodstream. Gliomas (astrocytoma) are the most common primary brain tumors. Forty to sixty percent of the primary brain tumors are gliomas. They originate from the star shaped glial cells (astrocytes) that support nerve cells. The symptoms of glioma are headaches, seizures or convulsions, difficulties in thinking or speaking, behavioral changes, loss of balance and vision changes. The treatment modalities of brain tumor include surgery, radiation therapy, immunotherapy and chemotherapy. Currently used chemotherapeutic agents suffer from major drawbacks of extremely severe toxicities like cardiotoxicity (carmustine), peripheral neuropathy (vincristine) and CNS depression (procarbazine). These limitations can partially be alleviated by use of a drug known for less severe side effects. However, majority of the chemotherapeutic agents are unable to cross the BBB and hence are not used for the treatment of brain tumor. Hence, there is a need to effectively deliver these safe chemotherapeutic agents to the brain.

Various strategies like enhancing the lipophilicity of the drugs, prodrugs, disruption of the BBB, carrier and receptor mediated drug delivery, colloidal drug delivery, alternative route of administration through the intranasal route have been explored for enhancing the drug delivery to brain.

Amongst the various strategies proposed for improving drug delivery to brain, the research on exploitation of nanoparticles as vectors is gaining impetus. Nanoparticles are used as transport vectors for delivery of many drugs to brain. Nanoparticles alter the characteristics and tissue distribution pattern of drug and allow the passage of the inaccessible drugs to the brain. Polymeric nanoparticles are interesting colloidal systems that allow the enhancement of therapeutic efficacy and reduction of toxicity of large variety of drugs. Nanoparticles of biodegradable polymers are safe and also provide prolonged release of the drug.

Additionally, the BBB is provided with active transport mechanisms like carrier mediated transport, adsorption mediated transport and receptor mediated transport for nutrient supply to the brain. Receptor mediated transport (RMT) employs the interaction of ligand with the receptors located at the luminal membrane, for the transport of nutrients across the BBB. Receptors localized at the BBB include the transferrin receptor, the insulin receptor, and the transporters for low-density lipoprotein, leptin and insulin-like growth factors. Transferrin receptor, a transmembrane glycoprotein, over-expressed on the BBB at the luminal end facilitates the delivery of iron to the brain through endocytosis of the iron binding protein transferrin. This receptor mediated transport mechanism can be useful for delivery of therapeutics to the brain. Surface engineering of the drug loaded polymeric nanoparticles by conjugation with transferrin alter the drug characteristics allowing its delivery across the BBB.

Alternatively, intranasal route delivers the drug rapidly and directly to brain by circumventing the BBB. The intranasal route has several advantages like non-invasive route of delivery, transport of the drug directly to brain with reduction in the drug delivery to the non target sites, reduction in the dosing and the associated site effects. The administration of nanoparticles through the intranasal route may not require the any ligand attachment or any surface modifier for delivery to brain.

Etoposide is a relatively safe chemotherapeutic agent, but the delivery of etoposide to brain is limited due to its physicochemical nature and in spite of more useful therapeutic application, it does not find role in brain tumour chemotherapy. Etoposide (ETP) {4'-Demethylepipodophyllotoxin 9-(4,6-O- (R)-Ethylidene- β -D-Glucopyranoside)}, is a semisynthetic derivative of podophyllotoxin with a molecular weight of 588.86 Da. Etoposide reported to be substrate PgP (MDR1) is effluxed at BBB and hence inadequately available in brain for treatment of brain tumours. Hence there is need for selective brain targeting of etoposide for use in effective treatment of brain tumor.

Temozolomide (TMZ) is currently used in the treatment of brain tumours. It undergoes rapid chemical conversion at physiologic pH to the active compound, monomethyl triazeno imidazole carboxamide (MTIC). However, temozolomide and MTIC both have short half-life of 1.5-2.0 hrs and require frequent administration for producing therapeutic response. Hence, delivering temozolomide encapsulated in nanoparticles will lead to the increased drug concentrations in brain by probable increase in the half-life.

The objective of the proposed work was to develop drug delivery system for effective treatment of brain tumor. Hence, ETP and TMZ were incorporated into polymeric PLGA nanoparticles and the surface of the nanoparticles was engineered by conjugation of transferrin and further characterized for particle size, entrapment efficiency, surface morphology and invitro drug release. The nanoparticles were evaluated for the invitro cytotoxicity on C6 glioma cells. The nanoparticles loaded with fluorescent dye were used to study their intracellular uptake. It was hypothesized that incorporation of the drugs in the nanoparticles will alter the pharmacokinetics of the drug making it long circulating and due to the presence of surface attached transferrin lead to targeted and enhanced delivery to the brain after intravenous administration. The efforts were made to deliver the nanoparticles through intranasal, for direct delivery to the brain bypassing blood brain barrier and for the cure of brain tumor or at least supplementary to parenteral therapy.

The estimation in the nanoparticles, invitro release studies for ETP and TMZ was performed by UV spectrophotometry and HPLC method respectively. The calibration curve of Etoposide was established in acetonitrile by UV spectrophotometry at 283nm. The linearity of Etoposide was found to be 5-120 μ g/ml ($R^2=0.9996$). The recovery studies for accuracy and precision were carried out at 10, 60 and 100 μ g/ml and the recovery was found to be more than 90%, indicating the reliability of the method. To determine the amount of drug entrapped nanoparticles were dissolved in acetonitrile. The resulting system was centrifuged to remove the precipitated components and the supernant was diluted with the solvent system and subjected to analysis.

The invitro release study was performed using the tube shaking method. At different time intervals, the samples were removed and centrifuged at 15000 rpm and the settled nanoparticles were dissolved in acetonitrile and analysed for the drug remaining in the nanoparticles as the same method for entrapment efficiency. The drug released was calculated by taking the difference of the drug taken initially and the drug remaining in the nanoparticles.

For Temozolomide, the calibration curve was established using HPLC with methanol: acetic acid (0.5%) (10:90) as mobile phase and detection at 330nm. The linearity of Temozolomide was found to be 1-25 μ g/ml ($R^2=0.9996$). The recovery studies for accuracy and precision were carried out at 2, 8 and 20 μ g/ml and the recovery was found to be more than 90%, indicating the reliability of the method. The drug entrapment efficiency and the invitro drug release were determined in the same manner as Etoposide, except that the drug was analysed using HPLC.

For cellular uptake experiments, a fluorescent dye 6-coumarin was incorporated into the PLGA nanoparticles and further conjugated with transferrin for enhanced uptake in the cell. 6-coumarin in the nanoparticles was estimated using spectrofluorimetric technique with excitation at 435nm and emission at 485nm. The calibration curve was established in acetonitrile and linearity was observed between 0.02-0.2 μ g/ml ($R^2= 0.998$). The recovery studies at 0.02, 0.08 and 0.15 μ g/ml showed greater than 90% recovery

The estimation of transferrin conjugation was carried out using BCA protein estimation. The calibration curve was established at 12.5-1000 μ g/ml ($R^2=0.9919$). The amount of PVA

associated with nanoparticles was determined by a colorimetric method based on the formation of a colored complex between two adjacent hydroxyl groups of PVA and an iodine molecule. A standard plot for known concentrations of PVA was established at 5-250 $\mu\text{g/ml}$. ($R^2=0.9997$)

The drug loaded nanoparticles were prepared by nanoprecipitation technique. The major process parameter effecting the formation of nanoparticles was the speed of the stirring. Evaluation of the variation of the stirring speed was carried out at slow, moderate and high speed. Moderate speed was optimized as the best suitable for the preparation of uniform nanoparticle dispersion. The rate of addition of organic phase to the aqueous was kept constant at 0.5ml/min throughout the entire experimentation. Based on preliminary investigations drug: polymer ratio, PVA concentration in aqueous phase (%w/v) and the ratio of the organic: aqueous phase were found to influence the major variables of particle size and entrapment efficiency. Hence, drug: polymer ratio (represented as polymer concentration, as the amount of the drug was kept constant), PVA concentration in aqueous phase (%w/v) and the ratio of the organic: aqueous phase (represented in decimal form) were kept as independent variables to find optimized condition to obtain lowest particle size (<150nm) with highest entrapment efficiency (dependent variables).

The particle size and entrapment were strongly influenced by the independent variables.

- The increase in the amount of PLGA (keeping the drug amount constant) resulted in the increase in the particle size of the nanoparticles. The viscosity of the organic phase in which the PLGA is dissolved appears to affecting the nanoparticles size due to hindrance in rapid dispersion of PLGA solution into the aqueous phase and resulted increase in the droplet and nanoparticle size. Increasing the polymer amount also increased the entrapment efficiency may be due to increase in drug entrapping polymer and due to the decrease in the diffusion of the drug towards the aqueous phase.
- Increase in the PVA concentration led to increase in the particle size of the nanoparticles. This increase in the nanoparticles size may be due to increase in the viscosity of the aqueous phase thereby increasing the resistance to the diffusion rate of the organic phase. The miscibility of organic phase (acetone) with aqueous phase results in orientation of PVA at the interface of PLGA solution in acetone present as

droplets in the system. Increase in PVA concentration also leads to increase in entrapment efficiency, probably due to reduction in diffusion rate of the organic phase in the aqueous phase.

- Increase in the ratio of organic phase: aqueous phase leads to decrease in the particle size and entrapment efficiency. The increase in the organic phase ratio leads increased evaporation time causing slower polymer precipitation, due to the increased microenvironment provided by organic phase after dispersing in the aqueous phase, and thereby formation of small particles. Due to the increased evaporation time and slower polymer precipitation, the tendency of the drug to escape in the aqueous phase before polymer precipitation increases leading to lower drug entrapment efficiency.

Twenty-seven batches for each ETP and TMZ nanoparticles were prepared by nanoprecipitation method by using 3^3 factorial design varying three independent variables drug: polymer ratio (X_1), %w/v PVA concentration (X_2) & organic: aqueous phase ratio (X_3). The PS and %EE were subjected to multiple regression analysis and mathematical modeling was done using second order polynomial equations (full model). Reduced model equations were achieved after neglecting the nonsignificant terms ($P > 0.05$). Results of analysis of variance (ANOVA) of full and reduced model demonstrated that the terms omitted from full model to achieve reduced model, were nonsignificant. The particle size and entrapment values for the 27 batches for ETP showed a wide variation starting from a minimum of 116nm to maximum of 186nm and minimum of 43.7% to maximum of 79.8% respectively. Similarly, for TMZ the particle size and entrapment values for the 27 batches ranged from minimum of 107nm to maximum of 181nm and minimum of 14.5% to maximum of 45.9% respectively

The reduced model was used for plotting the contour plots for particle size and entrapment efficiency. The contour plots were made by keeping the major contributing (variable with highest coefficient value) variable fixed. For ETP, the contour plots were made at fixed levels of -1, 0, and 1 of X_1 and the values of X_2 and X_3 between -1 to 1 for particle size and entrapment efficiency were computed. Similarly, for TMZ, the contours were plotted at fixed levels of -1, 0 and 1 of major contributing variable (X_1 for particle size and X_2 for entrapment efficiency). The contour plots demonstrate clearly the relationship between the independent

variable and dependent variables. The contour plots were used to predict the particle size and % entrapment efficiency. Three checkpoints were selected from contour plots, and the predicted values of particle size and % entrapment efficiency were compared with the experimental values using student t test. The difference was between the predicted and experimental values was found to be non-significant ($p > 0.05$). This proves the role of a derived reduced polynomial equation and contour plots in the preparation of nanoparticles of ETP and TMZ of predetermined PS and EE (%).

For Etoposide, the batch with particle size of 144 ± 6 nm and drug entrapment efficiency of 65.4 ± 2.2 % prepared at 0 level of X_1 (50mg polymer 5mg drug), 0 level of X_2 (1%w/v PVA in aqueous solution) and +1 level of X_3 (organic: aqueous phase of 1:2, i.e. 5ml of organic phase and 10ml of aqueous phase) was considered optimum based on the criteria of particle size < 150 nm with highest drug entrapment efficiency.

Similarly for temzolomide, the batch with 132 ± 4 nm particle size and 33.5 ± 1.1 % drug entrapment efficiency was considered to be optimum at the 0 level of X_1 (50mg polymer 5mg drug), 0 level of X_2 (1%w/v PVA in aqueous solution) and +1 level of X_3 (organic: aqueous phase of 1:2, i.e. 5ml of organic phase and 10ml of aqueous phase).

The optimized batch for Temozolomide was prepared by saturating the aqueous phase with Temozolomide before addition of the organic phase. By pre-saturation of the aqueous phase with Temozolomide the drug entrapment efficiency was enhanced to 70.3 ± 2.4 % with no change in particle size.

The optimized batch was subjected to lyophilization using sucrose, mannitol and trehalose as cryoprotectant at 1:1, 1:2 and 1:3 (nanoparticle: cryoprotectant). The redispersibility of the lyophilized product and particle size of the nanoparticles was measured after lyophilization. The redispersibility of nanoparticles with sucrose was poor and was only possible after sonication and show significant increase in particle size. The increase in the particle size could have been due to the cohesive nature of the sucrose. With mannitol, the redispersion was possible only after vigorous shaking and the particle size of the NPs increased on

lyophilization. This effect may be due to the low solubility of mannitol in water i.e. 0.18 part of mannitol soluble in 1 parts of water. With trehalose as cryoprotectant, the lyophilized nanoparticles were redispersed easily and the increase in particle size was not significant as indicated by Sf/Si of 1.04 for 1:3 of nanoparticles: trehalose. Also the tyndall effect was retained with use of trehalose as cryoprotectant. Hence, trehalose at a ratio of 1: 3 (nanoparticles: trehalose) was used as cryoprotectant for lyophilization of optimized batch of nanoparticles for further studies.

The prepared Etoposide nanoparticles (PLGA-ETP-NP) and temozolomide nanoparticles (PLGA-TMZ-NP) were conjugated with transferrin. Transferrin was conjugated to the nanoparticle surface in two steps involving the activation of the nanoparticles in the presence of catalyst zinc tetrafluoroborohydrate [$\text{Zn}(\text{BF}_4)_2$] with epoxy compound (SR-4GL, hexa epoxy) which acts as linker, followed by attachment of transferrin to the nanoparticle at the other end of the epoxy compound. PVA cross links with PLGA and is not removed despite several washings. In the conjugation process, atleast one of the epoxy of SR-4GL would have conjugated to the hydroxyl group of PVA and the other epoxy groups to the amine group of Tf. The amount of the activating agent (epoxy compound) and transferrin were optimized based on their influence on the particle size and surface transferrin density. The amount of the catalyst zinc tetrafluoroborohydrate [$\text{Zn}(\text{BF}_4)_2$] was kept constant at 5mg throughout the experiment.

The influence of the amount of epoxy compound on the density of surface Tf and particle size was evaluated keeping the amount of nanoparticles and the amount of Tf constant at 20mg and 10mg respectively. The amount of epoxy compound was varied at 5mg, 10mg and 20mg. With the increase in the amount of the epoxy from 5 to 10mg, the surface Tf density for Tf-PLGA-ETP-NP increased from 21.7 $\mu\text{g}/\text{mg}$ to 38.1 $\mu\text{g}/\text{mg}$ and the particle size increased from 154.5 nm to 162.1nm. Increasing further the epoxy compound to 20mg did not considerably increase the surface Tf density. However, the particle size increased from 162.1nm to 194 nm. Similar results were observed with Temozolomide nanoparticles. For TMZ the epoxy compound amount at 5, 10 and 20mg resulted in the surface Tf density of 19.6 $\mu\text{g}/\text{mg}$, 32 $\mu\text{g}/\text{mg}$ and 34.3 $\mu\text{g}/\text{mg}$ respectively, with corresponding particle size of 142nm, 153.8nm and 186nm. The

increase in the surface Tf density may be due to the increase in the number of the epoxy molecules reacting with hydroxyl of PVA and thereby increase in the availability of the epoxy groups for conjugation of Tf. The association of epoxy and Tf with nanoparticle is believed to have resulted in the increase in the particle size. Increasing the epoxy amount from 10mg to 20mg resulted in much increase in the particle size but the amount of the transferrin conjugated did not increase significantly. Hence, the epoxy amount was optimized at 10mg for both Etoposide and Temozolomide nanoparticles.

To study the influence of Tf added on the surface Tf density and particle size, different amount of Tf in solution were added to 20mg activated PLGA-ETP-NP and PLGA-TMZ-NP. The amount of Tf was varied from 2.5mg to 20mg. For PLGA-ETP-NP, with increase in the amount of Tf from 2.5 to 10mg, the surface Tf density increased from 16.1 μ g/mg to 38.1 μ g/mg and the particle size increased from 151nm to 162.1nm. Further increasing the amount of Tf from 10mg to 20mg, the Tf density increased from 38.1 μ g/mg to 46.4 μ g/mg. But the particle size increased from 162.1 to 312nm. Similarly for PLGA-TMZ-NP the surface Tf density and particle size were found to increase from 12.6 μ g/mg to 43.7 μ g/mg and 140nm to 290nm. With increase in the amount of Tf added for conjugation, the increase in the surface Tf density could have been due to the increase in the Tf molecule density available for conjugation. The increase in the particle size could have been due to increased surface Tf density. At the highest amount of Tf added for conjugation i.e 20mg, the particle size increased near to 300nm, probably due to the cross linking of Tf molecule with the epoxy groups of the neighboring molecules. For, intravenous administration, the preferable particle size is below 200nm and hence the 10mg Tf was considered as optimized amount.

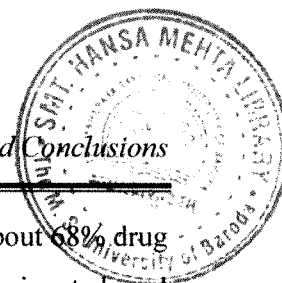
The amount of Tf was varied from 2.5mg to 20mg. For PLGA-ETP-NP, with increase in the amount of Tf from 2.5 to 20mg, the surface Tf density increased from 16.1 μ g/mg to 46.4 μ g/mg and the particle size increased from 149nm to 312nm. Similarly for PLGA-TMZ-NP the surface Tf density and particle size were found to increase from 12.6 μ g/mg to 43.7 μ g/mg and 140nm to 290nm. With increase in the amount of Tf added for conjugation, the increase in the surface Tf density could have been due to the increase in the Tf molecule density available for conjugation. The increase in the particle size could have been due to increased surface Tf

density. At the highest amount of Tf added for conjugation i.e 20mg, the particle size increased near to 300nm, probably due to the cross linking of Tf molecule with the epoxy groups of the neighboring molecules. For, intravenous administration, the preferable particle size is below 200nm and hence the 10mg Tf was considered as optimized amount.

The conjugation amino of Tf with the methylene of epoxy compound was confirmed by ^1H -NMR. For PLGA-ETP-NP and PLGA-TMZ-NP the peaks at 2.36 and 2.39ppm were observed representing the conjugation of amino group of Tf to the methylene group of epoxy compound.

The prepared nanoparticles were characterized for particle size, zeta potential, entrapment efficiency, invitro drug release. The surface morphology of the unconjugated and conjugated nanoparticles was assessed using Transmission Electron Microscopy. Residual PVA was determined using colorimetric reaction. Differential scanning calorimetry was to performed for ETP, PLGA-ETP-NP, TMZ, PLGA-TMZ-NP and PLGA to assess the state of drug present in the nanoparticles.

Surface conjugation with Tf leads to change in the particle characteristics. Conjugation with Tf increased the particle size from $149 \pm 8\text{nm}$ to $162.1 \pm 12\text{nm}$ and from $138 \pm 7\text{nm}$ to $153.8 \pm 14\text{nm}$ for Etoposide and Temozolomide nanoparticles respectively. The zeta potential changed from $-9.8 \pm 1.3\text{mV}$ to $-11.69 \pm 0.8\text{mV}$ and from -7.8 ± 1.7 to $-13.6 \pm 3.1\text{mV}$ for Etoposide and Temozolomide nanoparticles respectively. The % EE for PLGA-ETP-NP and Tf-PLGA-ETP-NP was determined to be $65.4 \pm 2.2\%$ and $57.7 \pm 3.1\%$ respectively. For PLGA-TMZ-NP and Tf-PLGA-TMZ-NP the %EE was determined to be $70.3 \pm 2.4\%$ and $61.4 \pm 2.9\%$ respectively. The reduction in the % EE after conjugation could be due to depletion of the surface associated drug, during the conjugation process. The release studies of etoposide and temozolomide were conducted in phosphate pH 7.4 + 0.1%w/v polysorbate-80 and phosphate buffer pH 7.4. For PLGA-ETP-NP there was an initial burst release of about 21% in 12hrs (0.5 days) and then there was a lag phase and about 80% release resulted in 21 days. The burst effect was absent in Tf-PLGA-ETP-NP and the release in 21 days was found to be about 60%. For PLGA-TMZ-NP the initial burst was about 27% in 12 hrs (0.5days) and lag phase showing about 75% release in 14days and further about 85% in 21 days. The cumulative drug



release for Tf-PLGA-ETP-NP was found to be devoid of initial burst and with about 68% drug release in 21 days. Transmission Electron Microscopy images of the unconjugated and conjugated NPs showed spherical NPs with smooth surfaces. Etoposide and Temozolomide demonstrate sharp melting peak at 279-289°C and 204.22-206.47°C respectively. In the nanoparticles the peak of Etoposide stretched from 239.7-294°C and the peak for temozolomide disappeared, indicating the presence of the drug in amorphous state or disordered-crystalline phase of a molecular dispersion or a solid solution state in the polymer matrix after nanoparticle formulation. The residual PVA associated with the nanoparticle surface was 7.8 ± 1.6 % & 7.2 ± 1.1 % w/w of nanoparticles for unconjugated etoposide and temozolomide nanoparticles and 5.7 ± 1.0 % & 5.2 ± 0.8 % w/w of nanoparticles for transferrin conjugated etoposide and temozolomide nanoparticles respectively.

Unconjugated and Tf conjugated fluorescent NPs encapsulating 6-coumarin required for studying cellular uptake of NPs by C6 glioma cells were prepared and characterized by the same methods used for drug loaded NPs. 6-coumarin loaded unconjugated NPs and Tf-conjugated NPs had a particle size of 151.6 ± 4 nm and 168.2 ± 9 nm and zeta potential of -7.9 ± 1.7 mV and -12.4 ± 1.2 mV respectively. Tf conjugated NPs had 34.1 µg Tf /mg of nanoparticles. The entrapment efficiency as evaluated using spectrofluorimetry was found to be 93.14 ± 2.71 and 85.48 ± 1.43 for unconjugated and conjugated 6-coumarin nanoparticles. The residual PVA was found to be 7.8 ± 2.0 % and 5.5 ± 1.5 % for unconjugated and transferrin conjugated nanoparticles respectively. The particle size, zeta potential, the surface density of Tf and residual PVA of 6-coumarin NPs were found to be similar to the drug loaded NPs. So it is expected that their cellular uptake would be similar to that of the drug loaded NPs.

The stability studies were conducted in accordance with ICH guidelines for drug products intended to be stored in a refrigerator. The stability of nanoparticle formulations in terms of particle size, zeta potential and drug content was conducted for 6 M at $5^{\circ}\text{C} \pm 3^{\circ}\text{C}$ and $25^{\circ}\text{C} \pm 2^{\circ}\text{C}/60 \pm 5$ % RH.

It was observed that unconjugated and conjugated nanoparticles of both Etoposide and Temozolomide there was no significant change ($P>0.05$) observed in particle size, zeta potential and drug content at $5^{\circ}\text{C} \pm 3^{\circ}\text{C}$ for 6M.

The storage of the unconjugated and conjugated nanoparticles of Etoposide and Temozolomide at $25^{\circ}\text{C} \pm 2^{\circ}\text{C}/60\% \pm 5\% \text{ RH}$, led to increase in the particle size. The increase in the particle size was not significant during the first month, however became significant and more prominent after 2, 3 and 6 months. During our analysis of samples, the polydispersity index of the nanoparticle stored at $25^{\circ}\text{C} \pm 2^{\circ}\text{C}/60\% \pm 5\% \text{ RH}$ was found to increase as compared to the initial. The increase in the particle size may be due to the absorption of the moisture by the nanoparticles resulting in the coalescence of the small nanoparticles forming particles larger in size.

The nanoparticles were also observed for physical appearance. After 3 and 6 months the physical appearance was also changed, with loss of the free flowing property followed by the difficulty in redispersibility. Also, the Tf conjugated nanoparticles demonstrated difference in the color than the initial powder. At 6 months the color of the powder was light pink. This could be indicative of the degradation of the surface transferrin.

At $25^{\circ}\text{C} \pm 2^{\circ}\text{C}/60\% \pm 5\% \text{ RH}$, the zeta potential of the nanoparticles shifted towards the zero for both unconjugated and conjugated nanoparticles. This may be due to the acidic conditions produced due to the degradation of PLGA into lactic and glycolic acid (Sanjeeb K. Sahoo et al, 2002). The lowered zeta potential values also might have contributed toward the aggregation of particles

The drug content of the unconjugated and conjugated nanoparticles was not altered upto 6M at $5^{\circ}\text{C} \pm 3^{\circ}\text{C}$. However, the drug content was reduced after 6M storage at $25^{\circ}\text{C} \pm 2^{\circ}\text{C}/60\% \text{ RH} \pm 5\% \text{ RH}$. The drug content for Temozolomide nanoparticles was found to have significant impact, with the drug content reducing below 95% after 3M and 6M storage at $25^{\circ}\text{C} \pm 2^{\circ}\text{C}/60\% \pm 5\% \text{ RH}$. This impact could be due to the moisture absorbed by the nanoparticles

upon storage at $25^{\circ}\text{C} \pm 2^{\circ}\text{C}/60\% \text{ RH} \pm 5\% \text{ RH}$, possibly resulting in the degradation of the drug.

Drug release evaluated for the 6M sample stored at $5^{\circ}\text{C} \pm 3^{\circ}\text{C}$ demonstrates not much difference in the release profile of the nanoparticles upon storage. The similarity factor calculated for the between the initial and the 6M samples show values greater than 80, indicating high similarity between the initial and 6M.

From the above study, we can demonstrate that the unconjugated and Tf-conjugated PLGA nanoparticles of Etoposide and Temozolomide when stored at $25^{\circ}\text{C} \pm 2^{\circ}\text{C}/60\% \text{ RH} \pm 5\% \text{ RH}$ for 6M show instability reflected by change in physical appearance, increase in the particle size, zeta potential and reduction in the drug content. Hence, we can conclusively specify that both unconjugated and conjugated nanoparticles of Etoposide and Temozolomide were stable and can be stored $5^{\circ}\text{C} \pm 3^{\circ}\text{C}$ for 6M retaining its original formulation characteristics.

Invitro cell culture studies were performed on C6 glioma cells to assess the intracellular nanoparticle uptake and to compare the antiproliferative action of the nanoparticles with the drug solution. C6 glioma cells were cultured and maintained as monolayer, growing as adherent monolayer in DMEM. DMEM was supplemented with 10% fetal bovine serum and 1% penicillin/streptomycin at 37°C in the atmosphere of 5% CO_2 and 95% relative humidity.

Intracellular uptake of the nanoparticles into the cell was studied by incorporating 6-coumarin (fluorescent dye) into the nanoparticles (PLGA-NP) and further conjugated with transferrin (Tf-PLGA-NP). Quantative intracellular uptake of the nanoparticles was performed to assess the influence of time and concentration. The nanoparticle cell uptake efficiency was found to increase with time from 0.5-4hrs for both the unconjugated and Tf conjugated nanoparticles. At all time points, the uptake efficiency of Tf conjugated nanoparticles was approximately 1.5~2 folds higher than the unconjugated nanoparticles. At 6hrs there was not much increase in the uptake efficiency for PLGA-NP suggesting the saturation of uptake with time. Hence, the influence of the concentration was performed keeping the incubation time at 4hrs for all concentrations.

Influence of the concentration was evaluated by incubating the cells for 4hrs at 50 $\mu\text{g/ml}$ -1000 $\mu\text{g/ml}$. The cellular uptake of the nanoparticles was observed to increase with increase in the concentration. However, the cellular uptake efficiency was found to be highest at the lowest concentration and found to decrease with increase in concentration. The decrease in the uptake efficiency indicates that the cells might have reached the saturating capacity for uptake. Tf-conjugated nanoparticles at all concentrations demonstrate 1.5-2 folds increased uptake over unconjugated nanoparticle uptake. The superior uptake of the Tf conjugated nanoparticles could be due to specific active endocytosis process mediated through the transferrin receptor. The receptor mediated uptake through transferrin receptor was confirmed by performing competitive uptake study, by previously incubating the cells with free Tf to the incubation medium. The addition of 50 μg free Tf to the incubation medium decreased the uptake efficiency of Tf conjugated nanoparticles by 20% during the time of the study.

The uptake of the nanoparticles in the cells was qualitatively confirmed by visualizing under fluorescent microscope. The fluorescent microscopic images showed green fluorescence in the cell cytoplasm and around the nucleus which reflects the internalization of the nanoparticles into the cell. Based on this observation, it is reasonable to believe that the nanoparticles may carry the active drug across the cell membrane into the cytoplasm. The Tf conjugated nanoparticles at all the time points demonstrated higher fluorescence intensity than the unconjugated nanoparticles confirming the results of the quantitative uptake studies. Also the Tf conjugated nanoparticles show higher number of the cells showing fluorescence than the unconjugated nanoparticles.

The cytotoxicity studies were performed using MTT assay. Cytotoxicity studies were performed at 1 μM -100 μM for Etoposide and 1 μM -200 μM for Temozolomide. The cytotoxicities of unconjugated and Tf conjugated nanoparticles were significantly ($p < 0.05$) higher than drug solution. The cytotoxicity was found to be dose and time dependent.

For Etoposide, the Tf conjugated nanoparticles produced significantly higher toxicities at all time points, i.e 24, 48, 72hrs, than the drug solution and unconjugated nanoparticles. After

24hrs, Tf conjugated nanoparticles at the higher concentrations showed superior toxicity differences compared to drug solution and unconjugated nanoparticles. An important observation was that with increase in incubation time at 72hrs, the lowest concentration (1 μ M) of Tf conjugated nanoparticles showed greater toxicity than drug solution and unconjugated nanoparticles. However, the higher concentrations didn't show much toxicity difference than the drug solution and unconjugated nanoparticles.

The cytotoxicity indicated by IC₅₀ values suggests that Tf conjugated nanoparticles at 24hrs are 1.73 and 2.30 time more cytotoxic than unconjugated nanoparticles and drug solution. These ratios increased to 2.63 and 6.66 for unconjugated nanoparticles; and 3.68 and 12 folds for drug solution at 48 hrs and 72 hrs respectively.

For Temozolomide, the cells treated with drug solution showed recovery of cells within 12 hrs indicated by increase in cell viability and did not produce any significant cytotoxic effect at any time point of 24, 48 and 72 hrs. At lowest concentration 1 μ M, even the unconjugated and transferrin conjugated nanoparticles did not product any cytotoxicity even after 72hrs. For all other concentrations (10-200 μ M) at all time points, Tf conjugated nanoparticles were found to be significantly toxic than unconjugated nanoparticles and drug solution.

For Temozolomide, no IC₅₀ was observed for the solution. The cytotoxicity indicated by IC₅₀ values suggests that Tf conjugated nanoparticles at 24hrs, 48 hrs and 72hrs are 2.2, 2.9 and 3.78 times more cytotoxic than unconjugated nanoparticles.

Etoposide is reported to be substrate of P-gp (expressed on C6 glioma cells), and hence would have been exocytosed leading to lower cytotoxicities. For Temozolomide, either the insufficient cytotoxic effect of the drug or due to the recovery of the cells could have led to insignificant cytotoxicity. The higher cytotoxicities with nanoparticles may be attributed to the enhanced intracellular levels of drug available after internalization of the nanoparticles. The superior cytotoxicity with Tf conjugated nanoparticles is due to the selective uptake of nanoparticles mediated through the transferrin receptors over expressed on C6 glioma cells.

The greater availability of the transferrin conjugated nanoparticles combined with the sustained release has led to the superior cytotoxicity.

The *in vivo* evaluation of the drug in solution and nanoparticles form was performed after radiolabeling with ^{99m}Tc . The drug solution and nanoparticle formulations were labeled with ^{99m}Tc with high labeling efficiency using direct labeling method. The radiolabeling was optimized for quantity of stannous chloride, incubation time. The quantity of stannous chloride and incubation time were optimized at 250 $\mu\text{g/ml}$ and 30mins for all the formulations of Etoposide and Temozolomide. For, Etoposide and formulations the pH was kept around 6.5 and for Temozolomide and formulations the pH was kept around 5.0. The labeling efficiency for ETPS, PLGA-ETP-NP and Tf-PLGA-ETP-NP was found to be 98.11%, 96.78% and 97.64 % respectively. The labeling efficiency for TMZs, PLGA-TMZ-NP and Tf-PLGA-TMZ-NP was found to be 97.23%, 96.69% and 97.17 % respectively. The radiolabelled complex show high stability in rat serum and 0.9%w/v sodium chloride with Radiolabeling efficiencies measured, greater than 90%. The DTPA challenging test, suggest high stability of the radiolabelled complex, with percent transchelation below 4%w/w at 50mM.

The *in-vivo* biodistribution studies were performed on Balb/c mice weighing between 25-30gms. The drug solution, unconjugated nanoparticles and Tf conjugated nanoparticles labeled with ^{99m}Tc were administered intravenously. The unconjugated nanoparticles were also administered intranasally in a different group. The studies were conducted for 24hrs and at different time intervals the radioactivity was measured in tissue/organ. The radioactivity in each tissue/organ was determined as fraction of administered dose per gram of the tissue (%A/g).

The radioactivity measured in the blood for unconjugated and Tf conjugated nanoparticles were significantly higher than the drug solution. For etoposide, at 24 hrs, the blood concentration of Tf conjugated nanoparticles and unconjugated nanoparticles were found to be 6.5 times and 4.78 times higher than drug solution. For Temozolomide, no radioactivity was detected in blood for drug solution after 24hrs. The unconjugated and conjugated nanoparticles depicted 0.83%A/g and 1.19%A/g. The higher radioactivity measured for

nanoparticles indicated increased residence time and slower elimination of drug from the nanoparticles. The increase in the residence time of the nanoparticles may be attributed to the smaller size of nanoparticle ($\leq 200\text{nm}$) of nanoparticles and hydrophilic surface imparted by the presence of the surface crosslinked PVA. The intranasal administration of the unconjugated nanoparticles for both etoposide and Temozolomide resulted in lower blood concentration than the intravenously administered nanoparticles.

The pharmacokinetic parameters of etoposide/temozolomide in mice after intravenous administration of drug solution and drug loaded nanoparticles including intranasal administration of unconjugated drug nanoparticles were calculated. Significant differences ($P < 0.05$) in results of various pharmacokinetic parameters were observed after intravenous administration of ETPS and Tf-PLGA-ETP-NP. The plasma $AUC_{(0 \rightarrow \infty)}$, MRT and $T_{1/2}$ of Tf-PLGA-ETP-NP were found to be significantly higher than etoposide solution. For Tf-PLGA-ETP-NP, the $AUC_{(0 \rightarrow \infty)}$, MRT and $T_{1/2}$ observed were respectively 5.15, 2.67 and 2.44 folds higher than ETPS. Similarly, Significant differences ($P < 0.05$) among results of various pharmacokinetic parameters were observed after intravenous administration of TMZS and Tf-PLGA-TMZ-NP. The plasma $AUC_{(0 \rightarrow \infty)}$, MRT and $T_{1/2}$ of Tf-PLGA-TMZ-NP were found to be significantly higher than temozolomide solution and unconjugated nanoparticles. For Tf-PLGA-TMZ-NP, the $AUC_{(0 \rightarrow \infty)}$, MRT observed were respectively 7.63, 7.45 folds higher than TMZS; and 1.44, 1.20 folds higher than the unconjugated nanoparticles. The $T_{1/2}$ for TMZ was observed to be 2.40 hrs as compared to 14.91 and 17.91 hrs for unconjugated and conjugated nanoparticles respectively. For both etoposide and temozolomide, the unconjugated nanoparticles administered intravenously demonstrated significantly higher $AUC_{(0 \rightarrow \infty)}$, MRT and $T_{1/2}$ than drug solution and intranasally administered unconjugated nanoparticles. The high values of MRT and $T_{1/2}$ for unconjugated and conjugated nanoparticles are indicative of slow clearance and long blood circulation of drug nanoparticles.

The major amount of the injected dose was found to accumulate in the organs of reticuloendothelial system comprising liver and spleen. For both Etoposide and Temozolomide, the distribution results show high accumulation of drug solution than unconjugated and Tf conjugated in liver. The low accumulation of nanoparticles may be due to

the hydrophilicity associated with the nanoparticle surface. Also, transferrin could have masked the recognition sites on the colloidal systems thereby reducing the liver uptake. The uptake of Etoposide nanoparticles in spleen was found to be higher than the drug solution. For Temozolomide, the drug solution depicted higher accumulation in spleen. After 24hrs, the radioactivity detected was higher for nanoparticles than drug solution. The retention of nanoparticles in the reticular fibre meshwork and the macrophages in red pulp of spleen may be attributed to this high accumulation.

For Etoposide and Temozolomide, the drug solution demonstrated higher activity than nanoparticle, in kidney indicating fast clearance of the drug solution. The nanoparticles compared to drug solution demonstrate higher radioactivity in lungs. The values of radioactivity for distribution to heart depict significantly higher values for solution than the nanoparticle formulation at all time points, indicating potential reduction in cardiotoxicity associated with drug using the nanoparticle formulation.

The radioactivity measured in the brain, for Etoposide and Temozolomide, indicates significantly higher accumulation of Tf conjugated nanoparticles than unconjugated nanoparticles and drug solution. For Etoposide, after 24hrs Tf conjugated nanoparticles exhibit 14 folds and 4.66 folds higher uptake in brain than plain drug and unconjugated nanoparticles respectively. For Temozolomide, at 24hrs the concentration of drug solution in brain recorded was not detectable. Tf conjugated nanoparticles at 24hrs show 4.75 folds higher uptake in brain than unconjugated nanoparticles.

The intranasal administration of unconjugated nanoparticles led to significantly superior brain deposition than the intravenous injection of same formulation and drug solution. At 24hrs, the brain concentration of intranasally administered nanoparticles was more than twice that of the same formulation administered intravenously. However, overall brain accumulation after intranasal administration of unconjugated nanoparticles was significantly lower when compared with intravenous injection of Tf conjugated nanoparticles.

The overall brain uptake ascertained from AUC_(0→24) brain indicates significantly higher uptake of Tf conjugated nanoparticles than the other groups. For ETP, the AUC_(0→24) brain for Tf-conjugated nanoparticles was calculated to be 11.29 folds and 4.69 folds significantly higher than drug solution and unconjugated nanoparticles after intravenous administration. When compared with intranasal administration of unconjugated nanoparticles, AUC_(0→24) brain for Tf-conjugated nanoparticles was 2.36 folds higher. However, unconjugated nanoparticles after intranasal administration exhibits significantly higher brain AUC_(0→24) at 1.98 folds and 4.77 folds compared to unconjugated nanoparticles and drug solution administered intravenously. For TMZ, the AUC_(0→24) brain for Tf-conjugated nanoparticles was calculated to be 8.56 folds and 4.79 folds significantly higher than drug solution and unconjugated nanoparticles after intravenous administration. When compared with intranasal administration of unconjugated nanoparticles, AUC_(0→24) brain for Tf-conjugated nanoparticles was 2.50 folds higher. However, unconjugated nanoparticles after intranasal administration exhibits significantly higher brain AUC_(0→24) at 1.92 folds and 3.43 folds compared to unconjugated nanoparticles and drug solution administered intravenously.

Poor brain uptake of etoposide solution is due to its inability to permeate across the BBB and it being substrate to Pgp (MDR1), efflux transporters, present at the blood brain barrier. Temozolomide due to low elimination half life is rapidly cleared from the blood leading to lower brain accumulation. For both etoposide and Temozolomide, the unconjugated and Tf conjugated nanoparticles bearing hydrophilic surface characteristic, due to the surface crosslinked PVA, could have led to increase in the residence time in blood and thereby leading to enhanced brain deposition. The preferential accumulation of Tf conjugated nanoparticles across the BBB may be the result of different events. The abundance of transferrin receptors on BBB could have resulted in the receptor mediated endocytosis, thereby transporting the particulates to the brain. Further, transferrin conjugated nanoparticles could have resulted in inhibition of multi drug resistance protein expressed on BBB, thereby preventing efflux of Tf-conjugated nanoparticles. Also, the actual condition of brain tumors leads to disruption of BBB, which may further enhance the better accumulation of the delivery system. The intranasal administration of unconjugated nanoparticles increased brain concentrations as compared to the intravenous administration of same formulation and drug solution. The

radioactivity detected in blood circulation after intranasal administration of unconjugated nanoparticles was significantly lower ($P < 0.05$) than the same formulation administered intravenously. This indicates the direct transport of the nanoparticles to the brain through the olfactory route bypassing the blood brain barrier.

The Gamma Scintigraphy imaging after 2hrs of intravenous administration of ^{99m}Tc labeled drug solution and nanoparticles of both etoposide and temozolomide was performed to ascertain the brain targeting qualitatively. The major radioactivity deposition is seen in liver and spleen, in confirmation to the biodistribution studies. The brain deposition shows higher accumulation of Tf conjugated in brain, following intravenous administration, as compared to unconjugated nanoparticles and drug solution is clearly depicted in the scintigram.

Conclusions

To conclude, PLGA loaded nanoparticles of etoposide were successfully prepared using nanoprecipitation method and conjugated with transferrin. The characterization of nanoparticles demonstrated small particle size ($< 200\text{nm}$) suitable for intravenous administration and drug release was found to be prolonged. The prepared nanoparticles were stable for 6M at refrigerated condition ($2-8^{\circ}\text{C}$) and demonstrated no significant change in particle size, drug content and invitro drug release compared to the initial. The intracellular uptake of nanoparticles loaded with fluorescent dye 6-coumarin showed significantly higher brain uptake with transferrin conjugated nanoparticles due to the receptor mediated uptake through the transferrin receptors located on the C6 brain glioma cells. The receptor mediated uptake was confirmed by competitive uptake of transferrin conjugated nanoparticles in presence of free transferrin. The antiproliferative studies on C6 brain glioma cells demonstrate significantly high cytotoxicity for transferrin conjugated nanoparticles compared to the unconjugated nanoparticles and drug solution. The cytotoxicity was found to be concentration and time dependent for drug solution, unconjugated and transferrin conjugated nanoparticles. Transferrin conjugated PLGA nanoparticles showed significantly improved brain uptake compared to unconjugated nanoparticles and drug solution after intravenous administration in mice. The improved drug uptake in the brain may be due to receptor mediated uptake mediated through transferrin receptors present in the blood brain barrier. The unconjugated

nanoparticles lead to higher brain uptake compared to drug solution and may be attributed to hydrophilic surface (PVA) of nanoparticles leading to increased blood circulation time. Almost similar results were observed with temozolomide. However, the drug solution of temozolomide showed no cytotoxic effect C6 brain glioma cells. The cells treated with drug solution were observed to recover within 12hrs indicating the phenomenon of cell repair and recovery. This effect may be due to the short half life of temozolomide and its active metabolite. The drug loaded nanoparticles and transferrin conjugated nanoparticles showed significantly higher and prolonged cytotoxicities compared to drug solution, probably due to intracellular conversion of the drug into active metabolite over a period of time. The improved and prolonged cytotoxicity of transferrin conjugated temozolomide PLGA nanoparticles suggest significantly higher and prolonged therapeutic response which may lead to reduction in dose/frequency of dosing and probably associated toxicities. This interesting finding encourages to further investigate this delivery system drug to possible clinical product. Transferrin conjugated PLGA nanoparticles showed significantly improved brain uptake compared to unconjugated nanoparticles and drug solution after intravenous administration in mice. The improved drug uptake in the brain may be due to receptor mediated uptake mediated through transferrin receptors present in the blood brain barrier. The unconjugated nanoparticles lead to higher brain uptake compared to drug solution and may be attributed to hydrophilic surface (PVA) of nanoparticles leading to increased blood circulation time. Significantly higher half life ($t_{1/2}$) and Mean Residence Time (MRT) were observed after intravenous administration of unconjugated and transferrin conjugated nanoparticles compared to drug solution.

The brain uptake of intranasally administered unconjugated nanoparticles was also observed to be significantly higher compared to intravenously administered etoposide nanoparticles or etoposide solution but was significantly lower compared to intravenously administered transferrin conjugated etoposide drug nanoparticles. Similarly for temozolomide, the intranasal administration of unconjugated PLGA nanoparticles leads to significantly higher brain uptake compared to intravenously administered temozolomide nanoparticles or drug solution but significantly lower brain uptake compared to intravenously administered transferrin conjugated

temozolomide drug nanoparticles. Faster and higher brain drug uptake after intranasal application may be due to direct nose to brain transport bypassing blood brain barrier.

The findings of these investigations suggest that etoposide in the form of transferrin conjugated nanoparticles can be effectively delivered to brain and may find a possible role in the treatment of brain tumor. The studies also suggest that delivering temozolomide in the form of transferrin conjugated nanoparticles enhances the brain uptake of the drug. The higher $t_{1/2}$ combined with prolonged release from nanoparticles can lead to possible reduction in the dose/frequency of dosing. However, more animal studies followed by extensive toxicological and clinical studies are necessary to confirm the role of Tf conjugated Etoposide/temozolomide loaded PLGA nanoparticles for the treatment of brain tumors.